Hindawi
International Journal of Aerospace Engineering
Volume 2023, Article ID 5429395, 12 pages
https://doi.org/10.1155/2023/5429395

Research Article

Identification of a Stochastic Dynamic Model for Aircraft Flight Attitude Based on Measured Data

Haiquan Li,[1] **Xiaoqian Chen**,[2] **Jiatu Zhang**,[3] **Bochen Wang**,[3] **Jiahui Peng**,[3] **and Liang Wang**[3]

[1]*College of Aerospace Science and Engineering, National University of Defense Technology, Changsha 410073, China*
[2]*National Innovation Institute of Defense Technology, Chinese Academy of Military Science, Beijing 100071, China*
[3]*Department of Applied Probability and Statistics, School of Mathematics and Statistics, Northwestern Polytechnical University, Xi'an 710129, China*

Correspondence should be addressed to Haiquan Li; lihaiquan601@163.com

Received 20 December 2022; Revised 7 August 2023; Accepted 29 September 2023; Published 28 October 2023

Academic Editor: Jiaying Zhang

Stochastic disturbances are everywhere. The influence of stochastic factors on the modeling and simulation of aircraft flight dynamics should be considered. Therefore, a stochastic differential equation for aircraft flight attitude is modeled based on the traditional one in this paper. After that, an identification method based on the idea of sparse recognition for unknown parameters and stochastic disturbance is proposed. Finally, a set of measured flight data is used to verify that the identified stochastic model has obvious advantages over the traditional deterministic model when the aircraft is maneuvering in flight. This method can improve the accuracy and reliability of the aircraft flight dynamic model.

1. Introduction

The flight dynamic model of the aircraft plays an important role in aircraft design. It can provide accurate and reliable data for aircraft modification design, flight control system optimization, ground simulation experiment, flight quality, and combat effectiveness evaluation. And it can reduce the number of costly and time-consuming flight tests and shorten the data processing time and the flight test cycle. However, the accuracy of the flight dynamic model is limited by complex aerodynamics. The system identification based on the measured flight data has provided technical support for improving the confidence of the model.

Modeling aircraft flight dynamics using the system identification method began in the 1950s. In 1951, Greenburg [1] and Shinbrot [2] first used the system identification method to study aircraft and proposed the least squares method to determine the stability derivative of aircraft based on flight tests.

Before the 1990s, the identification methods developed mainly include time domain identification and frequency domain identification. And the algorithm is no longer only for single-parameter identification; it has been developed to identify the structure of the model. The basic framework for model identification of aircraft flight dynamics has been gradually developed through the continuous efforts of scholars. This framework is roughly divided into the following three steps. First, the initial value of unknown parameters in the model is estimated. Second, the model structure is identified. Third, unknown parameters in the model are identified. Molusis [3] used the Kalman filter to identify the stability derivatives of helicopters. Kaletka [4] summarized the key technologies to be solved in the identification of the helicopter flight dynamic model system. Guy and Williams [5] identified the MK-50 Sea King helicopter by using the least squares method, the output error method, the maximum likelihood method, and the augmented

Kalman filter algorithm, which have been successfully applied to fixed-wing aircraft. Klein and Tischler et al. [6, 7] proposed the frequency domain identification algorithm of the helicopter, which was used for the flight dynamic model identification of the UH-60 helicopter. The development of frequency domain identification has laid a solid foundation for the identification of high-order flight dynamic models.

Since the 1990s, model identification has been mainly based on the high-order flight dynamic model, which has been extended to the nonlinear field at the same time. The identification accuracy and computational efficiency have been greatly improved. Most importantly, model identification has gone beyond the theoretical level to a variety of practical applications. Tischler and Cauffman et al. [8] developed a multiwindow spectrum optimization method to improve the accuracy of spectrum calculation and improve the identification ability of the high-order flight dynamic model. Jategaonkar and Plaetschke [9] carried out the early work of nonlinear model identification for BO-105 helicopter. Zhang et al. [10] proposed an aircraft's parameter identification algorithm, which optimizes the ML function with the cloud model optimization theory in accordance with the ML estimation principle, thus obtaining the values of the parameters to be identified. Majeed and Vikalp [11] build a neural model of an aircraft from flight data and online estimation of the aerodynamic derivatives from the established neural model. Bagherzadeh [12] provided a novel method that extracts observable flight modes from flight test data and uses them in the identification process by conducting a gray box time domain method. Wu and Chen [13] developed an online system identification method for tiltrotor aircraft flight dynamic modeling by establishing a weighted recursive least squares algorithm.

Simmons [14] established a mathematical model of the propulsion system by using the flight data of isolated propellers collected on the flight envelope line of aircraft. Ayyad et al. [15] proposed a new comprehensive method, DNN-MRFT, to complete the real-time identification and tuning of multirotor UAV. Rohr et al. [16] completed the modeling, system identification, and nonlinear model predictive control design of the longitudinal full envelope speed control of a small hybrid UAV. Ivler et al. [17] extracted the flight dynamic model of a hovering six-wing UAV through the state-space system identification method. Verma and Peyada [18] estimated and optimized unknown variables of the aircraft dynamic model by combining the recursive mechanism learning machine network and the Gauss-Newton method. Finally, the maximum likelihood method was used to verify estimated parameters and demonstrate the effectiveness of this method. Avcolu [19] identified and verified unknown aircraft aerodynamic parameters through an improved subspace identification method, and the identification results were satisfactory. Cao et al. [20] proposed system identification method based on interpretable machine learning for unknown aircraft dynamics. These model recognition methods are based on a definite model.

However, random noise is widely existed in practical problems and has an important effect on the real system [21–25]. Stochastic disturbance will affect simulation accuracy and efficiency and increase fragmentation, proximity, and shape complexity of simulation results [26, 27]. With the further improvement of the accuracy of aircraft flight dynamic model, it is necessary to consider the influence of stochastic factors on flight dynamics. In the study of infectious disease system identification, Tutsoy et al. [28] extended the SpID-N model as in the form of multi-input-multi-output structure by adding the multidimensional unknown uncertainties and proposed identification method of the system. For flight dynamic research, the calculation shows that the stochastic factors have a significant impact on the flight posture, and the stochastic response of the simulation model considering the uncertainty factors can more accurately simulate the flight state in the real environment than the deterministic response. Moreover, the existing deterministic identification methods cannot fully meet these requirements; stochastic identification methods came into being [29–32]. The main purpose of this paper is to identify the stochastic model of flight attitude dynamics based on the sparse identification algorithm and measured flight data.

The paper is organized as follows. In Section 2, we refine the deterministic model and obtain the stochastic model we studied. In Section 3, the identification procedure for the stochastic model obtained in Section 2 is fully showed. In Section 4, measured data of a particular type of aircraft is used as an example to validate the effectiveness of the method and the accuracy of the identified stochastic model. The concluding remarks are given in Section 5.

2. The Establishment of the Stochastic Model of Aircraft Flight Dynamics

2.1. The Traditional Deterministic Flight Attitude Dynamic Model. The traditional deterministic aircraft flight attitude dynamic model is a three-dimensional nonlinear motion equation, which is established under ideal assumptions. The deterministic model has good applicability when the aircraft is not subjected to any stochastic disturbance. However, the aircraft is inevitably affected by various stochastic loads, and this deterministic model is not enough to accurately describe the dynamic behavior of the aircraft in the actual flight. It can be used as prior information to provide some reference for the establishment of the stochastic model. The traditional deterministic model equation is shown in [32]

$$\begin{bmatrix} I_x\dot{\omega}_x \\ I_y\dot{\omega}_y \\ I_z\dot{\omega}_z \end{bmatrix} = \begin{bmatrix} M_x \\ M_y \\ M_z \end{bmatrix} + \begin{bmatrix} (I_y - I_z)\omega_y\omega_z \\ (I_z - I_x)\omega_z\omega_x \\ (I_x - I_y)\omega_x\omega_y \end{bmatrix}, \tag{1}$$

$$\begin{cases} M_x = \frac{1}{2}\rho v^2 SL\left(m_{x0} + m_x^{\beta}\beta + m_x^{\delta_x}\delta_x + m_x^{\delta_y}\delta_y + m_x^{\bar{\omega}_x}\bar{\omega}_x + m_x^{\bar{\omega}_y}\bar{\omega}_y\right), \\ M_y = \frac{1}{2}\rho v^2 SL\left(m_y^{\beta}\alpha + m_y^{\delta_y}\delta_y + m_y^{\bar{\omega}_y}\bar{\omega}_y + m_y^{\bar{\beta}}\bar{\beta} + m_y^{\bar{\delta}_y}\bar{\delta}_y\right), \\ M_z == \frac{1}{2}\rho v^2 SC\left(m_{z0} + m_z^{\alpha}\alpha + m_z^{\delta_z}\delta_z + m_z^{\bar{\omega}_z}\bar{\omega}_z + m_z^{\bar{\alpha}}\bar{\alpha} + m_z^{\bar{\delta}_z}\bar{\delta}_z\right). \end{cases} \tag{2}$$

where ω_x, ω_y, and ω_z are the angular velocity of the body shafting, respectively;I_x, I_y, and I_z are the moment of inertia of the aircraft on the body shafting, respectively; M_x, M_y, and M_z are the projection of the combined torque on the body shafting; L and S are the wingspan and reference area, respectively; C is the mean aerodynamic chord; ρ is the air density; α and β are the angle of attack and sideslip, respectively; δ_x, δ_y, and δ_z are the aileron angle, rudder angle, and elevator angle, respectively; $m_x^{\delta_x}$, $m_y^{\delta_y}$, and $m_z^{\delta_z}$ are manipulation derivatives; m_z^{α} and m_y^{β} are the statically stable derivatives; $m_x^{\omega_x}$, $m_y^{\omega_y}$, and $m_z^{\omega_z}$ are the derivatives of the damping moment and the derivatives of the washout time difference; and V is the velocity of the aircraft. For any variable x in this paper, the operator $\bar{x}$ stands for $\bar{x} = x \cdot (L/V)$.

This paper mainly studies axisymmetric aircraft, and it can be considered that the aircraft has no asymmetry between error and shape, that is, $m_{x0} = m_{z0} = 0$. In actual analysis, the influence of β, ω_y, and δ_y on M_x can be ignored. Similarly, the influence of $\dot{\bar{\beta}}$ and $\dot{\bar{\delta}}_y$ on M_y and influence of $\dot{\bar{\alpha}}$ and$\dot{\bar{\delta}}_z$ on M_z can be ignored; thus, Eq. (2) can be simplified to Eq. (3). A more detailed derivation is given in Ref. [33].

$$\begin{cases} M_x = \dfrac{1}{2}\rho V^2 SL\left(m_x^{\delta_x}\delta_x + m_x^{\omega_x}\omega_x\dfrac{L}{V}\right), \\ M_y = \dfrac{1}{2}\rho V^2 SL\left(m_y^{\beta}\beta + m_y^{\delta_y}\delta_y + m_y^{\omega_y}\omega_y\dfrac{L}{V}\right), \\ M_z = \dfrac{1}{2}\rho V^2 SC\left(m_z^{\alpha}\alpha + m_z^{\delta_z}\delta_z + m_z^{\omega_z}\omega_z\dfrac{L}{V}\right). \end{cases} \tag{3}$$

Among the above variables, aircraft ontology parameters, flight status parameters, flight environment data, and flight status parameters can be measured in real time by sensors and other equipment in the flight experiment process, while the aircraft ontology parameters and flight environment are set in the aircraft design process.

2.2. The Establishment of a Stochastic Flight Attitude Dynamic Model. In the previous section, the traditional model (Eq. (1)) of aircraft attitude dynamics is presented. A stochastic model is obtained by adding a random term to the torque term of the traditional model.

$$\begin{bmatrix} I_x\dot{\omega}_x \\ I_y\dot{\omega}_y \\ I_z\dot{\omega}_z \end{bmatrix} = \begin{bmatrix} M_x + I_x\eta_1(t) \\ M_y + I_y\eta_2(t) \\ M_z + I_z\eta_3(t) \end{bmatrix} + \begin{bmatrix} (I_y - I_z)\omega_y\omega_z \\ (I_z - I_x)\omega_z\omega_x \\ (I_x - I_y)\omega_x\omega_y \end{bmatrix}, \tag{4}$$

where M_x, M_y, and M_z are represented by Eq. (2).

Insight 1: the uncertainties in the actual situation are complex and diverse, and a stochastic model is obtained by adding a random term to the torque term of the deterministic model.

Insight 2: Eq. (4) is a stochastic differential equation. It is worth noting that stochastic terms $\eta_1(t)$, $\eta_2(t)$, and $\eta_3(t)$ are completely unknown. Unlike other identification methods that treat random items as Gaussian white noise, we do not make any assumptions about stochastic terms in advance.

Insight 3: on the right-hand side of Eq. (4), except for the stochastic terms $\eta_1(t)$, $\eta_2(t)$, and$\eta_3(t)$, the remaining terms can be obtained by in-flight experiments. The derivative term on the left-hand side of Eq. (4) needs to be solved by some methods, which will be covered in Section 3.

3. The Identification of the Stochastic Model of Aircraft Flight Dynamics

In this section, the actual measurement data of the aircraft and the traditional deterministic flight dynamic model (Eq. (1)) are taken as the priority information, and the process of constructing the flight dynamic stochastic model based on the sparse identification idea and the identification method of the model parameters is proposed.

3.1. TV Algorithm for Solving Derivatives. The derivative $\dot{X}$ in Eq. (10) of the measured data X is crucial for the identification of the stochastic model. The central difference method performs well for smooth data without disturbance. But during the actual flight, aircraft may be affected by stochastic factors such as air pressure, temperature, atmospheric density, turbulence, aircraft main parameters, and pilot control, which lead to random fluctuations in the attitude dynamics of the aircraft. Therefore, the derivatives of flight attitude data obtained by using the central difference method have great disturbance, and it is not satisfactory to use these derivatives for model identification.

In order to solve the problem, we can use total variation (TV) method to obtain the relatively smooth derivative values of the measured data. A brief introduction of TV algorithm is as follows.

In 1992, Rudin, Osher and Fatemi [34] first proposed the TV method, which can obtain relatively smooth derivative values without losing the jump information of the original data. The TV method needs to adjust the parameters so that the derivatives have good regularity. The derivative of the function f can usually be obtained by solving the following equation:

$$\min F(u) = \alpha R(u) + \mathrm{DF}(Au - f). \tag{5}$$

Here, $R(u)$ is the penalty term, $A(u) = \int_0^x u$ is the integral of u, and the upper limit x is a variable; in other words, the integral result $A(u)$ is the expression about x. α is a regularization parameter that controls the balance of the penalty term and fidelity term. $\mathrm{DF}(Au - f)$ is a data fidelity item, which tries to reduce the differences between Au and f. The data fidelity item is usually the square of L^2 norm, that is, $\mathrm{DF} = \int_0^L |\cdot|^2$.

The TV method solves the derivative of f in $[0, L]$ as the minimum of the function [35].

$$F(u) = \alpha\int_0^L \left|u'\right| + \frac{1}{2}\int_0^L |Au - f|^2. \tag{6}$$

We assume that $f \in L^2$ (a null hypothesis in the discrete case), and let $f(0) = 0$; F is defined in $\mathrm{BV}[0, L]$. Actually, F is continuous on $\mathrm{BV}(\mathrm{BV} \subset L^2)$, and it exists minimum value due to the compactness of BV on L^2 and the lower semicontinuous of BV seminorm. Meanwhile, F is strictly convex enough to ensure that F has a unique minimum u^*. A is the integral operator with a bounded kernel, and it is continuous on L^2.

3.2. The Identification Process of the Stochastic Model. The traditional identification method should traverse the functional basis composed of state variables to realize model identification. However, the method of traversing the basis will bring some problems to model identification. For example, going through all the functional basis will greatly increase the time cost of the computation. When the functional basis is less, the accuracy of the model may be insufficient. The model is more complicated when the functional basis is more. The sparse identification method can well balance the accuracy and complexity of the model [36].

Based on the idea of sparse identification, this paper establishes a stochastic model with the traditional deterministic model as the prior information. In this paper, ω_x, ω_y, ω_z, δ_{lx}, δ_{rx}, δ_y, δ_{lz}, δ_{rz}, ρ, α, β, V, and related combinations in model (1) are taken as the basis. Then, stochastic noise is introduced to build a stochastic flight dynamic identification model with unknown coefficients and unknown noises. The general form of the stochastic model is shown in

$$\begin{cases} I_x\dot{\omega}_x = a_1(I_y - I_z)\omega_y\omega_z + a_2\rho V^2\delta_{lx} + a_3\rho V^2\delta_{rx} + a_4\rho V\omega_x + I_x\eta_1(t), \\ I_y\dot{\omega}_y = b_1(I_z - I_x)\omega_x\omega_z + b_2\rho V^2\beta + b_3\rho V^2\delta_y + b_4\rho V\omega_y + I_y\eta_2(t), \\ I_z\dot{\omega}_z = c_1(I_x - I_y)\omega_x\omega_y + c_2\rho V^2\alpha + c_3\rho V^2\delta_{lz} + c_4\rho V^2\delta_{rz} + c_5\rho V\omega_z + I_z\eta_3(t), \end{cases} \tag{7}$$

where a_1, a_2, a_3, a_4, b_1, b_2, b_3, c_1, c_2, c_3, and $c_4$are the unknown parameters and $\eta_1(t)$, $\eta_2(t)$, and $\eta_3(t)$ are the independent stochastic disturbances. The meanings of the remaining parameters are given in Eq. (1).

Next, the stochastic model will be divided into a deterministic part and a stochastic perturbation part for identification, respectively. To facilitate description, the model is written in the following form:

$$\begin{aligned} &\dot{\Phi} = \widehat{\Phi} + \Phi^s, \\ &\begin{cases} \dot{\Phi} = \left[I_x\dot{\omega}_x\ I_y\dot{\omega}_y\ I_z\dot{\omega}_z\right]^T, \\ \widehat{\Phi} = \begin{bmatrix} a_1(I_y - I_z)\omega_y\omega_z + a_2\rho V^2\delta_{lx} + a_3\rho V^2\delta_{rx} + a_4\rho V\omega_x \\ b_1(I_z - I_x)\omega_x\omega_z + b_2\rho V^2\beta + b_3\rho V^2\delta_y + b_4\rho V\omega_y \\ c_1(I_x - I_y)\omega_x\omega_y + c_2\rho V^2\alpha + c_3\rho V^2\delta_{lz} + c_4\rho V^2\delta_{rz} + c_5\rho V\omega_z \end{bmatrix}, \\ \Phi^s = \left[I_x\eta_1(t) \quad I_y\eta_2(t) \quad I_z\eta_3(t)\right]^T, \end{cases} \end{aligned} \tag{8}$$

Table 1: Some parameters of an aircraft.

Symbol	Description	Numerical	Units
L	Wingspan	15.08	m
S	Wing area	70	m^2
I_x	Inertia moment	50000	$kg{\cdot}m^2$
I_y	Inertia moment	300000	$kg{\cdot}m^2$
I_z	Inertia moment	300000	$kg{\cdot}m^2$

where $\widehat{\Phi}$ denotes the deterministic part of the stochastic model (7) and Φ^s is the stochastic perturbation part. In the following, $\widehat{E} = \left[\widehat{\omega}_x \quad \widehat{\omega}_y \quad \widehat{\omega}_z\right]^T$ represents the measured data; $E = \left[\omega_x \quad \omega_y \quad \omega_z\right]^T$ represents the solution of $\dot{\Phi} = \widehat{\Phi}$; ΔE is the difference between E and $\widehat{E}$, that is, $\Delta E = \widehat{E} - E$, which represents the stochastic disturbance contained in the measured data; and $\Delta E = \left[\Delta\omega_x(t) \quad \Delta\omega_y(t) \quad \Delta\omega_z(t)\right]^T$ is recorded here.

The solution of equation $\dot{\Phi} = \widehat{\Phi}$ can well represent the dynamic behavior of aircraft flight without stochastic factors. Therefore, we firstly identify the unknown parameters in equation $\dot{\Phi} = \widehat{\Phi}$ based on the measured data $\widehat{E}$ and the least squares method. A brief introduction to the least squares method is as follows.

First, construct the data matrix:

$$\begin{aligned} \Phi_1 &= \left[\widehat{\omega}_y\widehat{\omega}_z \quad \widehat{\rho}\widehat{V}^2\widehat{\delta}_{lx} \quad \widehat{\rho}\widehat{V}^2\widehat{\delta}_{rx} \quad \widehat{\rho}\widehat{V}\widehat{\omega}_x\right], \\ \Phi_2 &= \left[\widehat{\omega}_x\widehat{\omega}_z \quad \widehat{\rho}\widehat{V}^2\widehat{\beta} \quad \widehat{\rho}\widehat{V}^2\widehat{\delta}_y \quad \widehat{\rho}\widehat{V}\widehat{\omega}_y\right], \\ \Phi_3 &= \left[\widehat{\omega}_x\widehat{\omega}_y \quad \widehat{\rho}\widehat{V}^2\widehat{\alpha} \quad \widehat{\rho}\widehat{V}^2\widehat{\delta}_{lz} \quad \widehat{\rho}\widehat{V}^2\widehat{\delta}_{rz} \quad \widehat{\rho}\widehat{V}\widehat{\omega}_z\right]. \end{aligned} \tag{9}$$

An important step in the sparse identification method is to select the correct model terms and construct data matrix. The general method is to extract the terms as the base according to some physical equations that the system may satisfy. The deterministic flight attitude dynamic model (Eq. (1)) can describe the flight attitude of the aircraft well without disturbance. Thus, it is credible to add the items contained in this deterministic model into the base library.

The equation $\dot{\Phi} = \widehat{\Phi}$ is split into overdetermined

$$\begin{cases} \dot{\widehat{\omega}}_x = \Phi_1\mathbf{a}, \\ \dot{\widehat{\omega}}_y = \Phi_2\boldsymbol{b}, \\ \dot{\widehat{\omega}}_z = \Phi_3\boldsymbol{c}, \end{cases} \tag{10}$$

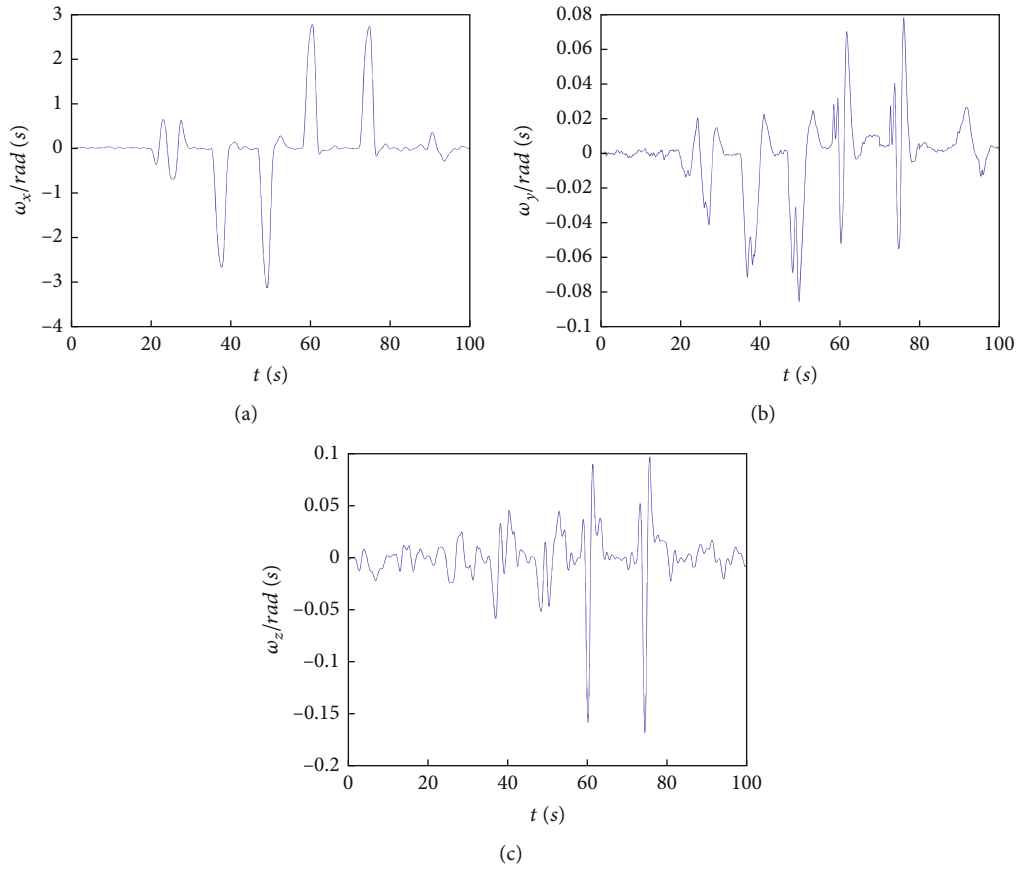

FIGURE 1: (a)–(c) represent the time history diagram of training data of angular velocity ω_x, ω_y, and ω_z, respectively.

where $\mathbf{a} = \begin{pmatrix} a_1(I_y - I_z) & a_2 & a_3 & a_4 \end{pmatrix}^T$, $\boldsymbol{b} = \begin{pmatrix} b_1(I_z - I_x) \\ b_2 b_3 b_4 \end{pmatrix}^T$, and $\boldsymbol{c} = \begin{pmatrix} c_1(I_x - I_y) & c_2 & c_3 & c_4 & c_5 \end{pmatrix}^T$. Solving Eq. (5) is equivalent to finding $\mathbf{a}$, $\boldsymbol{b}$, and $\boldsymbol{c}$, which satisfy

$$\begin{cases} \boldsymbol{a} = \arg \min_{\boldsymbol{a}} \left\| \dot{\hat{\omega}}_x - \Phi_1 \boldsymbol{a} \right\|_2, \\ \boldsymbol{b} = \arg \min_{\boldsymbol{b}} \left\| \dot{\hat{\omega}}_y - \Phi_2 \boldsymbol{b} \right\|_2, \\ \boldsymbol{c} = \arg \min_{\boldsymbol{c}} \left\| \dot{\hat{\omega}}_z - \Phi_3 \boldsymbol{c} \right\|_2. \end{cases} \tag{11}$$

The solution (12) of the system (10) can be simply expressed as Eq. (11) by using the optimal solution in the sense of two-norm.

$$\begin{cases} \boldsymbol{a} = \left({\Phi_1}^T \Phi_1 \right)^{-1} {\Phi_1}^T \dot{\hat{\omega}}_x, \\ \boldsymbol{b} = \left({\Phi_2}^T \Phi_2 \right)^{-1} {\Phi_2}^T \dot{\hat{\omega}}_y, \\ \boldsymbol{c} = \left({\Phi_3}^T \Phi_3 \right)^{-1} {\Phi_3}^T \dot{\hat{\omega}}_z, \end{cases} \tag{12}$$

where ${\Phi_i}^{-1}$ is the inverse of Φ_i and ${\Phi_i}^T$ is the transpose of Φ_i.

After obtaining equation $\dot{\Phi} = \hat{\Phi}$ with known parameters, we can get the behavior data E of aircraft without stochastic factors. Further, the stochastic disturbances contained in the measured data can be calculated by using equation $\Delta E = \hat{E} - E$. Note that model (7) is a differential equation, and ΔE is the increment of the disturbance part Φ^s of the stochastic model. It is worth mentioning that the Gaussian white noise is expressed as a formal derivative of the Wiener process. This expression is very common in the field of stochastic dynamical systems. The stochastic process usually does not have strictly mathematical theoretical derivatives; its formal derivative is typically expressed as a noise. In this paper, ΔE is the increment of the stochastic response within a sampling time interval Δt, and Φ^s is a formal derivative of the stochastic process, which can be referred to as noise. To sum up, the relationship between ΔE and Φ^s can be expressed as

$$\begin{aligned} \frac{\Delta E}{\Delta t} &= \frac{\begin{bmatrix} \Delta\omega_x(t) & \Delta\omega_y(t) & \Delta\omega_z(t) \end{bmatrix}^T}{\Delta t} \\ &= \Phi^s = \begin{bmatrix} I_x \eta_1(t) & I_y \eta_2(t) & I_z \eta_3(t) \end{bmatrix}^T. \end{aligned} \tag{13}$$

After the above steps are performed, the aircraft flight stochastic dynamic model can be identified. In the following, we will demonstrate the effectiveness of our method through the numerical example.

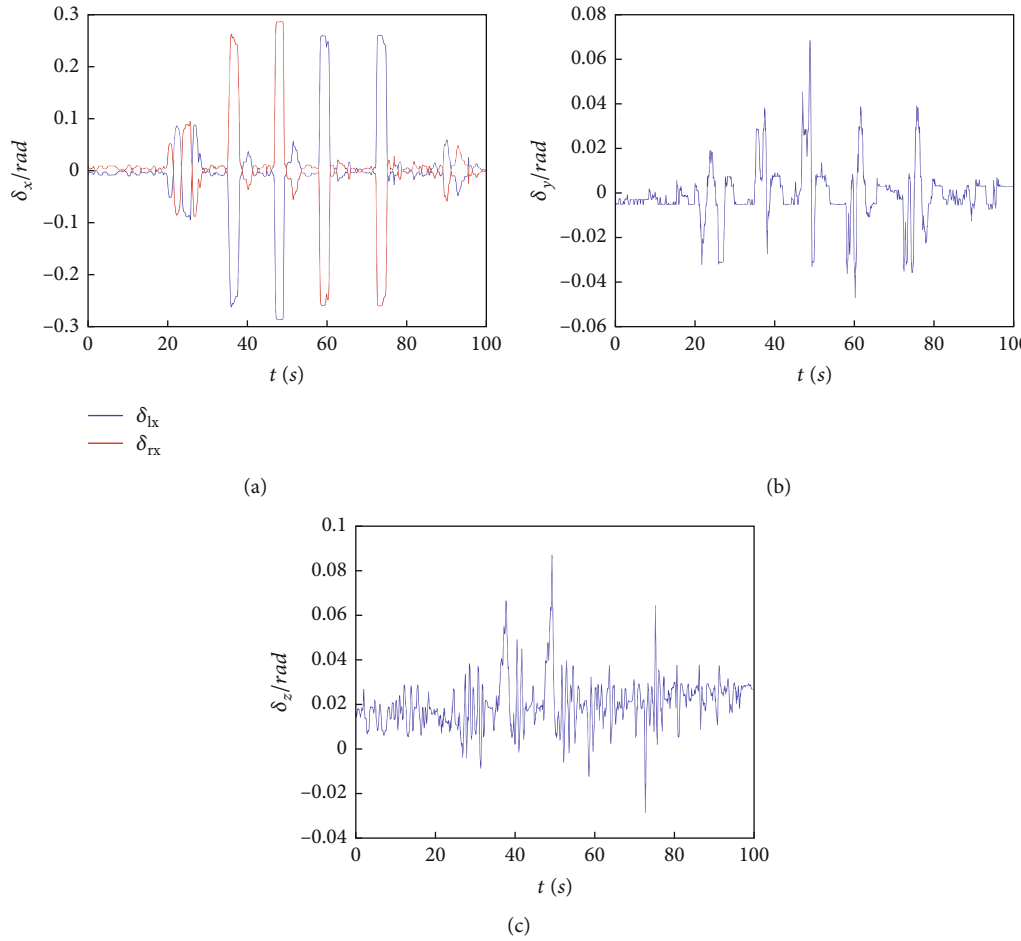

Figure 2: (a)–(c) represent the time history diagram of training data of rudder angle δ_x, δ_y, and δ_z, respectively.

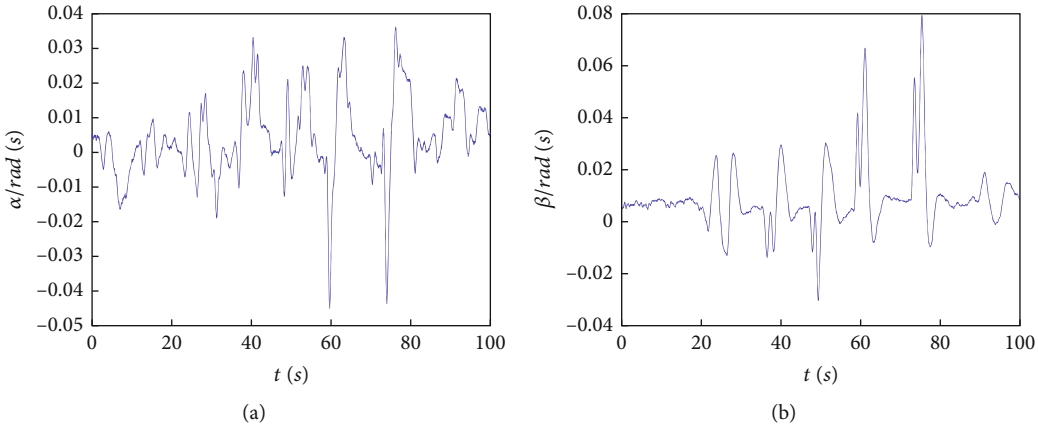

Figure 3: (a) and (b) represent the time history diagram of training data for attack angle α and sideslip angle β, respectively.

4. Numerical Example

In this section, we will illustrate the identification process in actual application and demonstrate the effectiveness of our method on the basis of actual data from a certain type of aircraft.

4.1. Real Data Preprocessing. Some parameters of this aircraft are shown in Table 1. Next, the stochastic model is identified based on the measured flight data, and the sampling frequency of the measured data here is 32 Hz. The measured data is divided into training data and prediction data. The training data is used to identify the stochastic

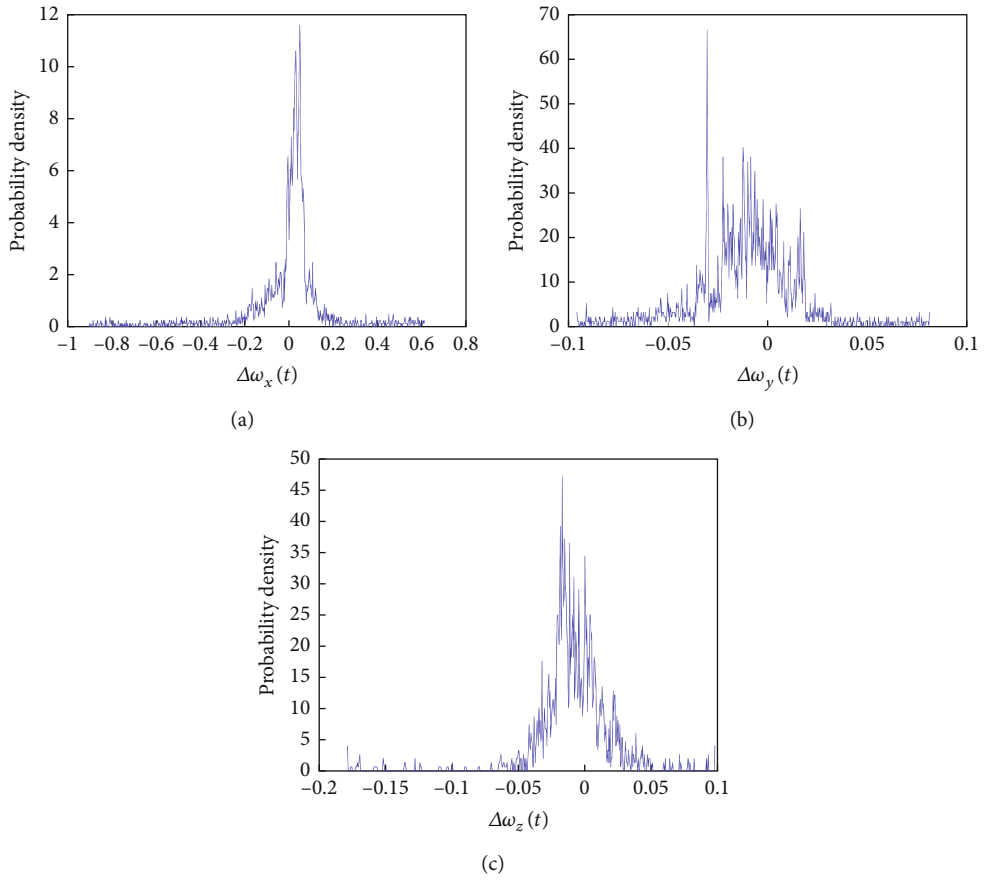

FIGURE 4: (a)–(c) represent the probability density plots of the stochastic disturbance $\Delta\omega_x(t)$ contained in ω_x, $\Delta\omega_y(t)$ contained in ω_y, and $\Delta\omega_z(t)$ contained in ω_z, respectively.

model, and the prediction data is used to verify the effectiveness of the identified model.

Figure 1 is the time history diagrams of the training data of the angular velocity component of the aircraft. Figure 2 draws the time history diagrams of the training data of the three rudder declination angles according to the measured data. Figure 3 represents the time history diagram of training data for the attack angle α and sideslip angle β.

In addition, according to the actual situation, the rudder deflection angles δ_{lx} and δ_{rx} of the aircraft during flight should be roughly symmetric about 0, and δ_{lz} and δ_{rz} should be roughly equal. However, the measured data show different characteristics, which may be caused by measurement errors such as the accuracy of the measuring instrument. In order to make the model identified closer to reality, the rudder deflection angles δ_{lx} and δ_{rx} were slightly shifted to make them roughly symmetric about 0, and δ_{lz} and δ_{rz} were equal through $\delta_z = 1/2(\delta_{lz} + \delta_{rz})$. After data processing, the training data $\widehat{E}$ used for model identification are shown in Figures 1 and 2.

Finally, it should be noted that when the least squares method is used to identify the parameters of the equation, it is necessary to solve the derivative of angular velocity. For the data without noise, the central difference can be used to solve this problem. However, the measured data contains a lot of random information, and the direct derivation will lead to large fluctuations in the derivative value. Therefore, the TV algorithm mentioned in the previous section is combined to obtain the derivative of ω_x, ω_y, and ω_z.

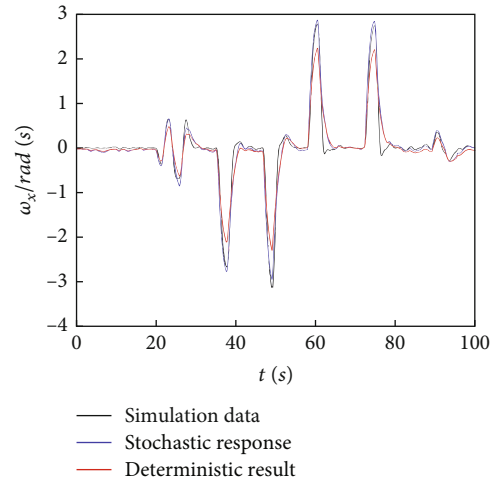

FIGURE 5: Comparison plot of solution results of ω_x.

4.2. The Identification of the Stochastic Model. First, we identify the deterministic part $\dot{\Phi} = \widehat{\Phi}$ of Eq. (7) based on $\widehat{E}$ and the least squares method. The identification results of the equation $\dot{\Phi} = \widehat{\Phi}$ using the TV algorithm and the least squares method are as follows.

$$\begin{cases} I_x\dot{\omega}_x = 43.297\rho v^2\delta_{lx} - 43.297\rho v^2\delta_{rx} - 1956.074\rho v\omega_x, \\ I_y\dot{\omega}_y = -0.584\omega_x\omega_z + 8.683\rho v^2\beta - 5.245\rho v^2\delta_y - 612.120\rho v\omega_y, \\ I_z\dot{\omega}_z = 0.477\omega_x\omega_y + 4.489\rho v^2\alpha + 0.374\rho v^2(\delta_{lz} + \delta_{rz}) - 126.454\rho v\omega_z. \end{cases} \tag{14}$$

Then, the fourth-order Runge-Kutta method is used to solve the deterministic part Eq. (5). In order to keep consistent with the sampling frequency 32 Hz of the measured data, the fourth-order Runge-Kutta iterative step is selected $\Delta t = 1/32$. Thus, we can obtain solutions of ω_x, ω_y, and ω_z by numerically solving Eq. (14). Then, the difference between the training data $\widehat{\omega}_x$, $\widehat{\omega}_y$, and $\widehat{\omega}_z$ and the simulation results ω_x, ω_y, and ω_z can be used to obtain the probability density function of stochastic disturbances $\Delta\omega_x(t)$, $\Delta\omega_y(t)$, and $\Delta\omega_z(t)$, as shown in Figure 4, respectively.

We can carry out numerical simulation of stochastic disturbances $\Delta\omega_x(t)$, $\Delta\omega_y(t)$, and $\Delta\omega_z(t)$ by the probability density function of stochastic disturbances. Then, the stochastic model (15) can be obtained by using $\left[\begin{array}{ccc} I_x\eta_1(t) & I_y\eta_2(t) & I_z\eta_3(t) \end{array}\right] \approx 1/\Delta t\left[\begin{array}{ccc} \Delta\omega_x(t) & \Delta\omega_y(t) & \Delta\omega_z(t) \end{array}\right]$.

$$\begin{cases} I_x\dot{\omega}_x = 43.297\rho v^2\delta_{lx} - 43.297\rho v^2\delta_{rx} - 1956.074\rho v\omega_x + I_x\eta_1(t), \\ I_y\dot{\omega}_y = -0.584\omega_x\omega_z + 8.683\rho v^2\beta - 5.245\rho v^2\delta_y - 612.120\rho v\omega_y + I_y\eta_2(t), \\ I_z\dot{\omega}_z = 0.477\omega_x\omega_y + 4.489\rho v^2\alpha + 0.374\rho v^2(\delta_{lz} + \delta_{rz}) - 126.454\rho v\omega_z + I_z\eta_3(t). \end{cases} \tag{15}$$

4.3. Numerical Simulation of the Stochastic Model. To verify the accuracy of the identified model, we solve the dynamic response of this model (15). It should be emphasized that the response of the stochastic system is different from the solution of the deterministic model. The response of a stochastic system is a stochastic process (or a stochastic variable), which cannot be directly compared with the measured data. Therefore, we consider extracting the numerical characteristics of the stochastic response, that is, the sample means, and comparing it with the deterministic result and training data to show whether the stochastic system can more accurately describe the actual flight problem.

The comparison diagrams of numerical simulation results of flight dynamic responses ω_x, ω_y, and ω_z with measured data $\widehat{\omega}_x$, $\widehat{\omega}_y$, and $\widehat{\omega}_z$ are, respectively, drawn below. The red line represents the solution result of the deterministic model (1). The blue line represents the solution of stochastic model (15). The black line represents measured training data.

It can be seen from Figures 5–7 that ω_y and ω_z only show small fluctuations, while ω_x rolls due to the pilot's control in the actual flight process. Small fluctuations may be caused by small changes in the environment, such as height, temperature, or wind, and such stochastic factors have relatively little influence on the response of the system. The large fluctuations are caused by the pilot's large maneuvering action, which has a great influence on the flight dynamic behavior of the aircraft. Therefore, we mainly analyze the solution result of ω_x, which contains more complex stochastic information.

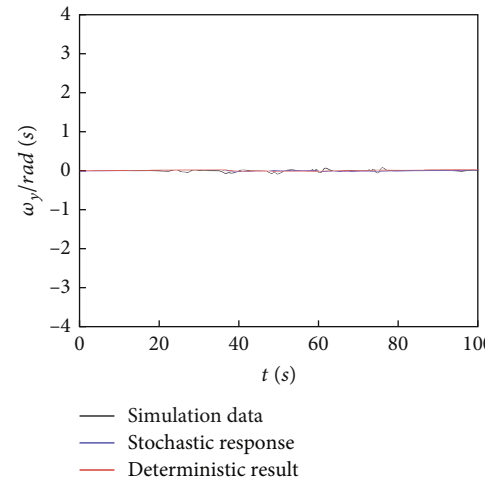

Figure 6: Comparison plot of solution results of ω_y.

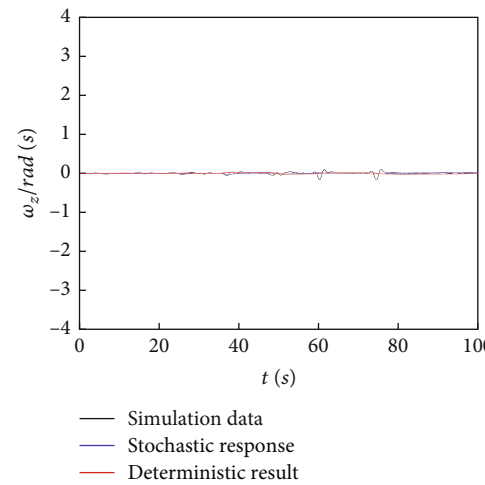

Figure 7: Comparison plot of solution results of ω_z.

Table 2: The mean square error analysis of the solution results of the stochastic model, the deterministic model, and the measured training data.

	The deterministic model	The stochastic model
ω_x	0.1930	0.0685

Figures 5–7 show the comparison of solution results of the deterministic model, stochastic model, and measured training data. It can be seen that the simulation result of the stochastic model is more precise than that of the deterministic model when the aircraft is maneuvering. However,

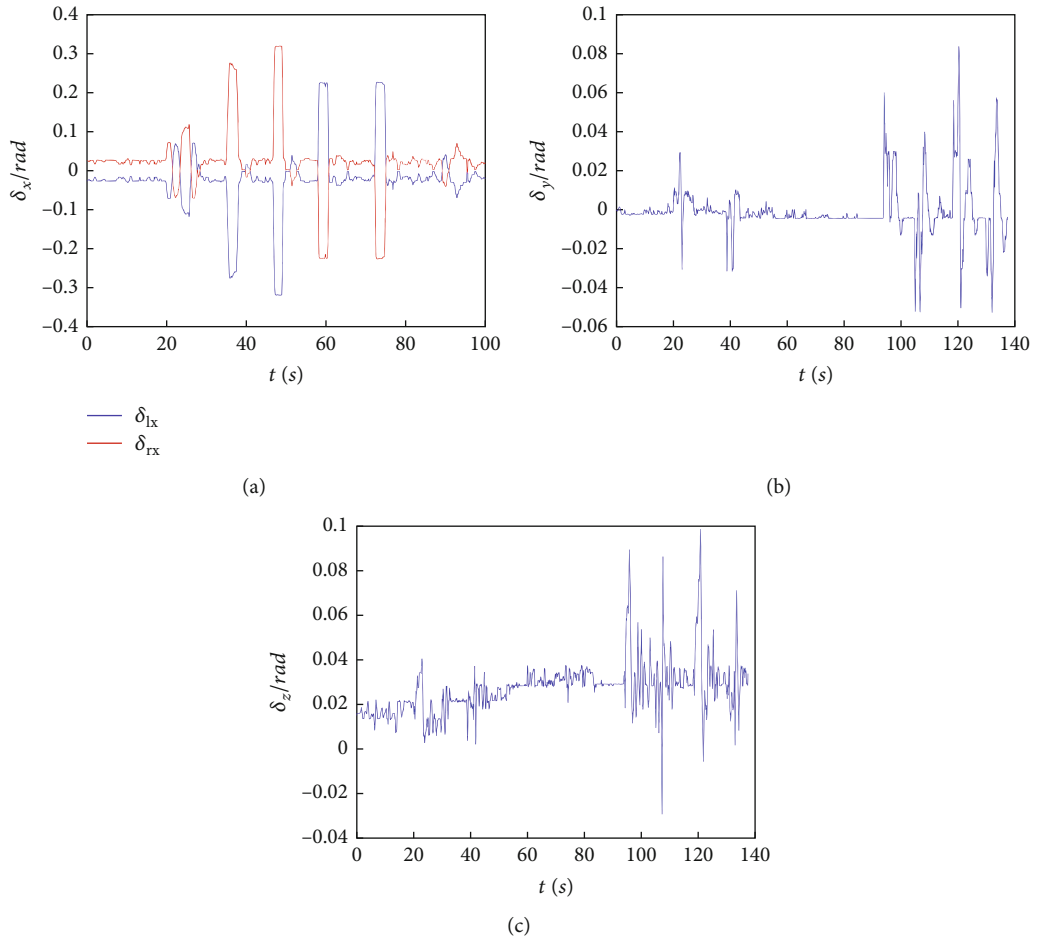

Figure 8: (a)–(c) represent the time history diagram of predicted data of rudder angles δ_x, δ_y, and δ_z, respectively.

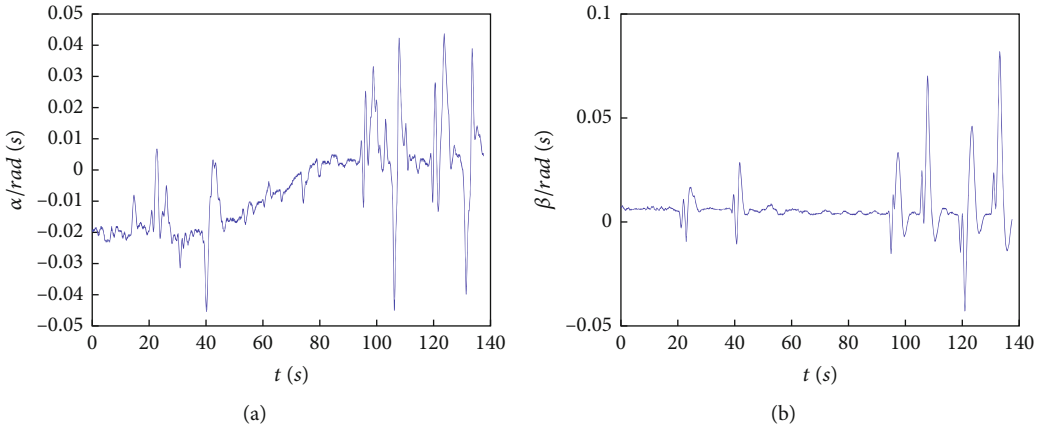

Figure 9: (a) and (b) represent the time history diagram of predicted data for the attack angle α and sideslip angle β, respectively.

there are some errors between the results of the stochastic model and deterministic model and the measured training data. After all, the stochastic result is the average value of multiple groups of samples, while the measured data is only one group of samples. It is difficult to ensure that the sample has the same value as the mean, but the mean can well reflect the characteristics of the sample. The error analysis table of the solution results of the stochastic model and deterministic model and training data is given below to observe the advantages of the stochastic model from qualitative and quantitative perspectives. The stochastic model shows good simulation results in the case of aircraft maneuvering flight. The mean square error of the solution results and the measured training data is calculated when $0.5 < \omega_x$.

As can be seen from Table 2, the accuracy of the solution results of the stochastic model is significantly improved

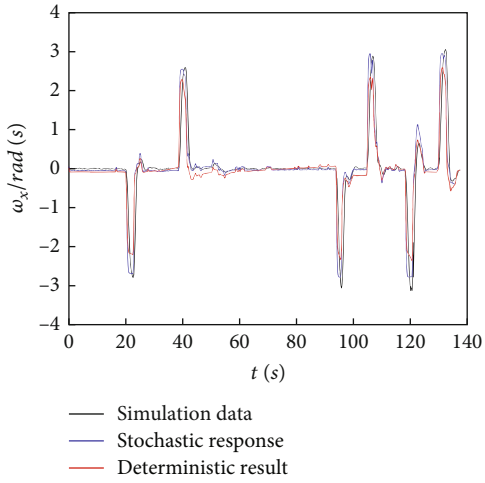

Figure 10: Comparison of the predicted results of ω_x.

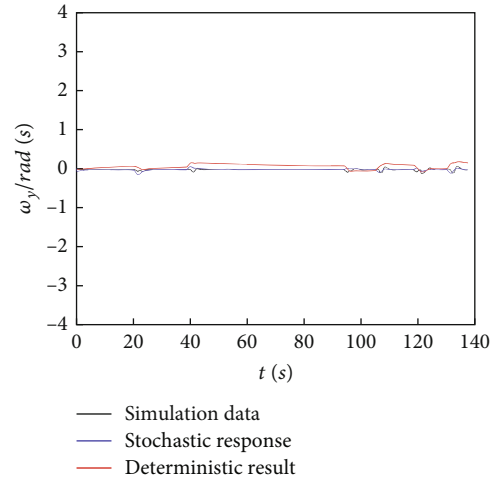

Figure 11: Comparison of the predicted results of ω_y.

compared with that of the deterministic model. From the value of the mean square error, the mean square error of the stochastic model pair is obviously smaller than that of the deterministic model. This shows that the stochastic model has good accuracy from a quantitative point of view.

The above comparison between the solution results of the stochastic model and the measured training data shows the accuracy of the stochastic model and the effectiveness of the algorithm in this paper. To further confirm the robustness of the stochastic model (15), its ability to predict the flight attitude of the same aircraft will be verified below.

4.4. Prediction Results of the Stochastic Model. In this section, the stochastic model (15) will be used to predict the flight attitude of the aircraft in a certain period, and the prediction results of the model will be compared qualitatively and quantitatively with the measured data to further illustrate the practicality of the stochastic model (15).

Figures 8 and 9 show the data required by stochastic model (15) to predict flight attitude ω_x, ω_y, and ω_z. Figures 8(a)–8(c) show the time history diagrams of predicted data representing the rudder angles δ_x, δ_y, and δ_z, respectively, and Figures 9(a) and 9(b) represents the attack angle α and sideshow angle β, respectively. Then, the stochastic Runge-Kutta method was used to solve the dynamic response of model (15), and the iteration step was still 0.01.

The comparison diagram of the predicted results ω_x, ω_y, and ω_z and measured data is drawn below. The red line represents the solution result of the traditional deterministic model (1). The blue line represents the prediction results of the stochastic model (15). The black line represents the measured data.

The results of Figures 10–12 show that the prediction results of the stochastic model fit well with the flight measured data when the aircraft rolls. However, the prediction results of the traditional deterministic model (1) have great errors with the flight measured data. In particular, the comparison is particularly obvious at the larger maneuvering peak in Figure 10. The prediction results of the stochastic

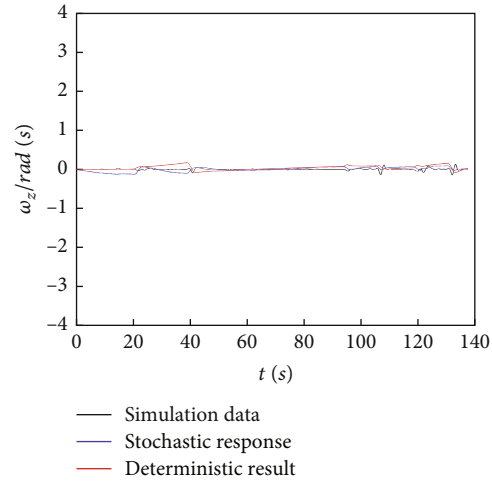

Figure 12: Comparison of the predicted results of ω_z.

Table 3: The mean square error analysis of the solution results of the stochastic model, the deterministic model, and the measured predicted data.

	The deterministic model	The stochastic model
ω_x	1.0844	0.7463

model are closer to the measured data, while the solution results of the deterministic model have a large error, which highlights the higher accuracy of the stochastic model when the aircraft does large maneuvers.

Table 3 shows the comparison of the mean square error of the solution results of the deterministic model, the stochastic model, and the measured predicted data. From the numerical perspective, it can be seen that the stochastic model has better prediction ability. From a quantitative point of view, the stochastic model is closer to reality than the deterministic model, which further confirms the

effectiveness of the recognition algorithm and the good robustness of the stochastic model.

In general, the stochastic model is more close to the measured data from qualitative and quantitative perspectives. The stochastic model shows more precise prediction results compared with the deterministic model when the aircraft is rolling. Therefore, the model considering stochastic factors is more consistent with the real flight state and can effectively improve the reliability of flight dynamic simulation model.

5. Conclusion

In this paper, we use the idea of sparse identification to establish the stochastic model of flight attitude dynamics. Based on the measured data of aircraft flight attitude dynamics containing stochastic disturbances, the stochastic model is divided into the deterministic part and random disturbance part for identification, respectively, and then, the stochastic model of flight dynamics is obtained by using the least squares method. Furthermore, we compare and analyze the solutions of the stochastic model and the traditional deterministic model with the measured data, respectively. The comparison results show that the calculation results of the stochastic model are in good agreement with the measured data, especially when the aircraft is maneuvering in flight, and the stochastic model has obvious advantages compared with the traditional deterministic model. This demonstrates that the algorithm in this paper is effective for the identification of stochastic models driven by measured data. It also shows that it is necessary to consider the influence of stochastic factors when modeling and simulating aircraft flight dynamics.

Data Availability

Data will be made available by contacting the corresponding author.

Conflicts of Interest

The authors have declared that no competing interests exist.

Authors' Contributions

All authors contributed equally to this work.

Acknowledgments

This work is supported by the National Natural Science Foundation of China (Grant No. 11972289).

References

[1] H. Greenburg, *A Survey of Methods for Determining Longitudinal-Stability Derivatives of an Airplane from Transient Flight Data*, NACA-TN-2340, 1951.

[2] M. Shinbrot, *A Least Squares Curve Fitting Method with Applications to the Calculate on of Stability Coefficients from Transient-Response Data*, NACA-TN-2341, 1951.

[3] J. A. Molusis, *Helicopter Stability Derivative Extraction and Data Processing Using Kalman Filtering Techniques*, American Helicopter Society National Forum, Washington D.C, 1972.

[4] J. Kaletka, *Rotorcraft Identification Experience*, AGARD LS-104, 1979.

[5] C. R. Guy and M. J. Williams, "Flight testing of an ASW helicopter," *Vertica*, vol. 9, no. 4, pp. 465–480, 1985.

[6] V. Klein, *Maximum Likelihood Method for Estimating Airplane Stability and Control Parameters from Flight Data in Frequency Domain*, NASA TP-1637, 1980.

[7] M. B. Tischler, J. G. M. Leung, and D. C. Dugan, "Frequency-Domain Identification of XV-15 Tilt-Rotor Aircraft Dynamics in Hovering Flight," in *AIAA/AHS 2nd Flight Testing Conference*, Las Vegas, 1983.

[8] M. B. Tischler and M. G. Cauffman, "Frequency-response method for rotorcraft system identification: flight applications to BO-105 coupled fuselage/rotor dynamics," *Journal of the American Helicopter Society*, vol. 37, no. 3, pp. 3–17, 1992.

[9] R. Jategaonkar and E. Plaetschke, *Maximum Likelihood Parameter Estimation from Flight Test Data for General Non-Linear System*, DLR-FB-8314, 1983.

[10] W. Zhang, Y. L. Liu, D. P. Guo, K. Masood, and J. Tian, "An aircraft's parameter identification algorithm based on cloud model optimization," in *2014 14th International Conference on Control, Automation and Systems (ICCAS 2014)*, Gyeonggi-do, Korea, 2014.

[11] M. Majeed and D. Vikalp, "Aircraft neural modeling and parameter estimation using neural partial differentiation," *Aircraft Engineering and Aerospace Technology*, vol. 90, no. 5, pp. 764–778, 2018.

[12] B. S. Amin, "Flight dynamics modeling of elastic aircraft using signal decomposition methods," vol. 233, no. 12, pp. 4380–4395, 2019, Proceedings of the Institution of Mechanical Engineers Part G Journal of Aerospace Engineering.

[13] W. Wu and R. L. Chen, "An improved online system identification method for tiltrotor aircraft," *Aerospace Science and Technology*, vol. 110, article 106491, 2021.

[14] B. M. Simmons, "System identification for propellers at high incidence angles," *Journal of Aircraft*, vol. 58, no. 6, pp. 1336–1350, 2021.

[15] A. Ayyad, M. Chehadeh, P. H. Silva et al., "Multirotors from takeoff to real-time full identification using the modified relay feedback test and deep neural networks," *IEEE Transactions on Control Systems Technology*, vol. 30, no. 4, 2020.

[16] D. Rohr, M. Studiger, T. Stastny, N. R. J. Lawrance, and R. Siegwart, "Nonlinear model predictive velocity control of a VTOL tiltwing UAV," *IEEE Robotics and Automation Letters*, vol. 6, no. 3, pp. 5776–5783, 2021.

[17] C. M. Ivler, E. S. Rowe, J. Martin, M. J. S. Lopez, and M. B. Tischler, "System identification guidance for multirotor aircraft: dynamic scaling and test techniques," *Journal of the American Helicopter Society*, vol. 66, no. 2, pp. 1–ss, 2021.

[18] H. O. Verma and N. K. Peyada, "Estimation of aerodynamic parameters near stall using maximum likelihood and extreme learning machine-based methods," *The Aeronautical Journal*, vol. 125, no. 1285, pp. 489–509, 2021.

[19] S. Avcolu, A. T. Kutay, and K. Leblebiciolu, "Identification of physical helicopter models using subspace identification," *Journal of the American Helicopter Society*, vol. 65, no. 2, pp. 1–14, 2020.

[20] R. Cao, Y. P. Lu, and Z. He, "System identification method based on interpretable machine learning for unknown aircraft dynamics," *Aerospace Science and Technology*, vol. 126, article 107593, 2022.

[21] I. Bashkirtseva, S. Fedotov, L. Ryashko, and E. Slepukhina, "Stochastic bifurcations and noise-induced chaos in 3D neuron model," *International Journal of Bifurcation and Chaos*, vol. 26, no. 12, article 1630032, 2016.

[22] Y. X. Zhang and W. D. Wang, "Mathematical analysis for stochastic model of Alzheimer's disease," *Communications in Nonlinear Science and Numerical Simulation*, vol. 89, article 105347, 2020.

[23] E. Slepukhina, L. Ryashko, and P. Kugler, "Noise-induced early afterdepolarizations in a three-dimensional cardiac action potential model," *Chaos, Solitons & Fractals*, vol. 131, article 109515, 2020.

[24] F. Yang, Y. Y. Zheng, J. Q. Duan, L. Fu, and S. Wiggins, "The tipping times in an Arctic sea ice system under influence of extreme events," *Chaos*, vol. 30, no. 6, article 063125, 2020.

[25] B. H. Wang, Q. S. Lu, and S. J. Lv, "The spatio-temporal stochastic resonance of calcium in coupled hepatocytes systems affected by subthreshold stimuli and noise," *Acta Physica Sinica*, vol. 58, no. 11, pp. 7458–7465, 2009.

[26] B. Zhang, H. Wang, S. He, and C. Xia, "Analyzing the effects of stochastic perturbation and fuzzy distance transformation on Wuhan urban growth simulation," *Transactions in GIS*, vol. 24, no. 6, pp. 1779–1798, 2020.

[27] J. M. Ma, X. Y. Zhan, and S. K. Zeng, "Performance reliability analysis method of dynamic systems under stochastic processes," *Systems Engineering and Electronics*, vol. 33, no. 4, pp. 943–948, 2011.

[28] O. Tutsoy, K. Balikci, and N. F. Ozdil, "Unknown uncertainties in the COVID-19 pandemic: multi-dimensional identification and mathematical modelling for the analysis and estimation of the casualties," *Digital Signal Processing*, vol. 114, article 103058, 2021.

[29] W. Yao, X. Chen, W. Luo, M. van Tooren, and J. Guo, "Review of uncertainty-based multidisciplinary design optimization methods for aerospace vehicles," *Progress in Aerospace Sciences*, vol. 47, no. 6, pp. 450–479, 2011.

[30] Z. Qian, W. Weijun, and Q. Xiangju, "Method for analyzing the influence of random factors in carrier launching," in *AIAA atmospheric flight mechanics conference*, p. 4643, Minneapolis, Minnesota, 2012.

[31] H. Guocai, X. Guang, W. Yunliang, and L. Shuyan, "Model of airflow field on the deck for shipborne helicopter flight dynamics analysis," *Transactions of Nanjing University of Aeronautics and Astronautics*, vol. 34, no. 5, pp. 567–577, 2017.

[32] L. Haiquan and C. Xiaoqian, "The research on the stochastic dynamics of the aircraft flight attitude," *Acta Aeronautica et Astronautica Sinica*, vol. 43, no. 1, article 125232, 2022.

[33] X. F. Zhang, *Modeling and simulation of the flight vehicle dynamics for motion simulation*, Beijing Jiaotong University, Beijing, 2014.

[34] L. I. Rudin, S. Osher, and E. Fatemi, "Nonlinear total variation based noise removal algorithms," *Physica D*, vol. 60, no. 1-4, pp. 259–268, 1992.

[35] R. Chartrand, "Numerical differentiation of noisy, nonsmooth data," *ISRN Applied Mathematics*, vol. 2011, Article ID 164564, 11 pages, 2011.

[36] S. H. Rudy, S. L. Brunton, J. L. Proctor, and J. N. Kutz, "Data-driven discovery of partial differential equations," *Science Advances*, vol. 3, no. 4, article e1602614, 2017.